Steady state temperature distribution in Human Skin during burn injury using The Finite Element Method with Bio-Heat Equation

Md. Matiar Rahman [a], Nazmun Nahar Papri [b], Mridul Sannyal [c], Abul Mukid Mohammad Mukaddes [c] and Aminur Rahman Khan [d]

[a] Department of Mathematics, Shahjalal University of Science and Technology, Sylhet, Bangladesh.

[b] Department of Civil Engineering, Leading University, Sylhet, Bangladesh.

[c] Department of of Industrial and Production Engineering, Shahjalal University of Science and Technology, Sylhet, Bangladesh.

[d] Department of Mathematics, Jahangirnagar University, Savar, Dhaka, Bangladesh.

E-mail: mmrahman-mat@sust.edu, npapri21@gmail.com, mridul.sust.ipe@gmail.com, mukaddes1975@gmail.com, aminur@juniv.edu

Abstract:

Human skin is exposed to high thermal energy due to solar radiation, contact with a hot disk, contact with hot fluid etc. This high thermal energy may result in the thermal burn. Depending upon the excess thermal energy and exposure duration, burn injury can be severe and may lead to damage of the skin. Prior knowledge of the temperature distribution in the skin burn is thus necessary for the proper treatment of the skin burn injuries. In this study a 2D Finite Element (FE) model of human skin in contact with a heating disk is developed. Natural convection to ambient air and evaporation boundary condition is considered to the area that is not in direct contact with the heating disk. Whether, temperature boundary condition is considered at the body core. A C program is developed for the solution of the finite element model. Linear and quadratic triangular element is used for the analysis. FEM result was compared with commercial numerical solver (COMSOL-Multiphysics) and boundary element method. A good agreement was found. The effect of various parameters i.e. ambient temperature, ambient heat transfer coefficient, blood perfusion, evaporation rate, disk temperature is briefly discussed for the temperature distribution of human skin.

Keywords: Finite Element Method, Pennes Equation, Bio heat transfer, Skin Burn, Burn Integral.

*Author for correspondance e-mail: mmrahman-mat@sust.edu

1. INTRODUCTION

Burns are a global public health problem. It is estimated that nearly 265000 people die each year due to burn injuries [1]. The main cause of burns is the deposition of excess thermal energy into biological bodies. Different parameters contribute thermal energy that causes burns, for example, radiation, an electric source, contact with chemicals, hot objects, and hot fluid. Depending on the severity of the burn, it is classified as first degree, second degree, or third degree. Third-degree burns are very dangerous, and the consequence is death. For many years, researchers have been attempting to determine the temperature at which burn occurs. They suggest that the human body can undergo heat up to 430 °C without any damage [2]. So damage starts due to excess thermal energy beyond 43^0C. Both the exposed temperature and exposure duration contribute equally to the burn severity. Soon after the Second World War, much of the research that led to the development of a mathematical model to predict burns occurred. Henriques and Moritz were among them [3]. The usage of Henriques' burn integral was supported by Buettner [4]. Experimental study of biological systems during heating is very difficult and costly, so mathematical modelling is widely used in engineering problems to model the temperature distribution in human body during burning. Due to complex geometry heaving three different layers of skin with different material properties an analytical solution is very difficult to obtain. Hence arises the necessity of numerical modelling. Advances in computation technology allow the accurate prediction of tissue temperature during a burn. The heat transfer in the biological tissue is governed by the well-known Pennes bio-heat equation [5]. Though, initially this bio-heat equation was developed to predict heat transfer in human forearm later it was implemented in various biological research works. This equation is used in skin bio-heat transfer by [6-8]. Bio-heat equation for two dimensional can be defined as

$$c\rho \frac{\partial T}{\partial t} = \left\{ \frac{\partial}{\partial x}\left(k\frac{\partial T}{\partial x} \right) + \frac{\partial}{\partial y}\left(k\frac{\partial T}{\partial y} \right) + \omega_b \rho_b c_b \left(T_\alpha - T \right) \right\} + Q_m \qquad (1)$$

Mathematical model used Pennes bio-heat equation for knowing the temperature distribution in human skin can be found in [9-13]. In this paper, two-dimensional finite element model has been developed to compute the temperature distribution in human skin. Also, C programming language is developed to compute the temperature distribution in this model.

2. HUMAN SKIN MODEL

The human skin is usually modeled as a three-layered region in the axis symmetric coordinate system XOY . The epidermis Ω_1 (the outermost layer), dermis Ω_2 (the middle layer), and subcutaneous fat Ω_3 (the deepest layer) are the three regions taken into account along X-axis. A heating disk with a constant temperature was used on the epidermis surface along Y-axis. Natural convection to ambient air and evaporation boundary condition is considered to the area that is not in direct contact with the heating disk. This is shown in Fig. 1.
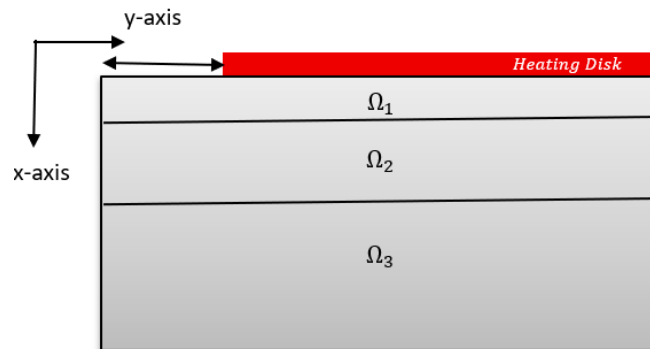

Fig. 1- The human skin model.

2.1 THE GOVERNING EQUATION

Two dimensional steady state Pennes Bio-heat Equation [6] is defined as

$$\left\{ \frac{\partial}{\partial x}\left(k\frac{\partial T}{\partial x}\right) + \frac{\partial}{\partial y}\left(k\frac{\partial T}{\partial y}\right) + \omega_b \rho_b c_b \left(T_\alpha - T\right)\right\} = 0 \qquad (2)$$

Where k, and ρ represent the tissue thermal conductivity, and density respectively, ρ_b, c_b denote density

and specific heat of blood; ω_b denotes the blood perfusion; T_a denotes the known arterial temperature, T denotes unknown tissue temperature, and the metabolic heat generation has been considered negligible.

2.2. THE ASSOCIATE BOUNDARY CONDITIONS

$$T = T_b \text{ on } \Gamma_3, \quad T = T_d \text{ on } \Gamma_2, \quad -k\frac{\partial T}{\partial x} = 0 \quad \text{on} \quad \Gamma_4,$$

$$-k\frac{\partial T}{\partial x} = 0 \text{ on } \Gamma_5, \quad -k\frac{\partial T}{\partial x} = h_b\left(T - T_0\right) + E \quad \text{on } \Gamma_1$$

Here E, h_b, T_b, T_d and T_0 are the evaporation rate, heat convection coefficient, the core body temperature, the temperature of disk and ambient temperature respectively.
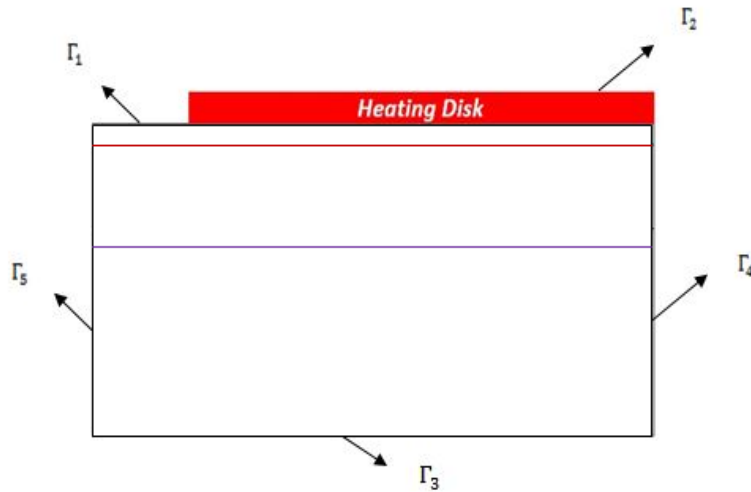

Fig. 2- Model and Boundary Conditions

2.3. NUMERICAL IMPLEMENTATION

The governing equation has the weak form [14]

$$\int_\Omega^{\square} w\left[-\left\{ \frac{\partial}{\partial x}\left(k\frac{\partial T}{\partial x}\right) + \frac{\partial}{\partial y}\left(k\frac{\partial T}{\partial y}\right)\right\} + CT - f\right] dxdy = 0 \qquad (3)$$

where $C = \omega_b \rho_b c_b$, $f = C T_a$ and w is a waight function.

Applying gradient (Divergence theorem)

$$\int_{\Omega} -w \frac{\partial}{\partial x}\left(k \frac{\partial T}{\partial x}\right) dxdy = \int_{\Omega} k \frac{\partial w}{\partial x} \frac{\partial T}{\partial x} dxdy - \oint_{\Gamma} wk \frac{\partial T}{\partial x} \eta_x \, ds$$

$$\int_{\Omega} -w \frac{\partial}{\partial y}\left(k \frac{\partial T}{\partial y}\right) dxdy = \int_{\Omega} k \frac{\partial w}{\partial y} \frac{\partial T}{\partial y} dxdy - \oint_{\Gamma} wk \frac{\partial T}{\partial y} \eta_y \, ds$$

Now Eq. (3) reduces to

$$\int_{\Omega}\left[k \frac{\partial w}{\partial x} \frac{\partial T}{\partial x} + k \frac{\partial w}{\partial y} \frac{\partial T}{\partial y} + CwT - wf\right] dxdx - w \oint_{\Gamma}\left(k \frac{\partial T}{\partial x} \eta_x + k \frac{\partial T}{\partial y} \eta_y\right) ds = 0 \qquad (4)$$

For convective boundary, the natural boundary condition is a balance of energy transfer across the boundary due to conduction and/ or convection (i.e., Newton's law of cooling):

$$k \frac{\partial T}{\partial x} \eta_x + k \frac{\partial T}{\partial y} \eta_y + \beta\left(T - T_{\infty}\right) = \hat{q}_n \qquad (5)$$

where β is theconvective heat transfer coefficient in W m^{-20}C^{-1}, T_{∞} is the ambient temperature, and $\hat{q}_n$ is the specific heat flow. The first two terms account for heat transfer by conduction, the third term for heat transfer by convection, while the term on the right hand side accounts for specific heat flux. The boundary integral should be modified to account for the convective heat transfer term. We use Eq. (5) in the weak form ($\hat{q}_n$ is replaced by q_n, which is obtained o n the element boundary) that is in Eq. (4) and we obtain

$$\int_{\Omega} k \frac{\partial w}{\partial x} \frac{\partial T}{\partial x} + k \frac{\partial w}{\partial y} \frac{\partial T}{\partial y} + CwT - wf \,] dxdy - w \oint_{\Gamma}\left[q_n - \beta\left(T - T_{\infty}\right)\right] ds = 0 \qquad (6)$$

Using quadratic approximation function as $T_h^e(x) = \sum_{j=1}^{e} \varphi_j^e(x) T_j^e$.

The finite element model of the governing equation is

$$\sum_{j=1}^{n}\left\{\int_{\Omega^e}\left[\left(k \frac{\partial \psi_i^e}{\partial x} \frac{\partial \psi_j^e}{\partial x} + k \frac{\partial \psi_i^e}{\partial y} \frac{\partial \psi_j^e}{\partial y} + C \psi_i^e \psi_j^e\right) dxdy + \oint_{\Gamma^e} \beta \psi_i^e \psi_j^e ds\right] T_j^e - \int_{\Omega^e} f \psi_i^e dxdy - \oint_{\Gamma} \psi_i^e \beta T_{\infty} ds - \oint_{\Gamma} \psi_i^e q_n ds\right\} = 0$$

(7)

Simplifying Eq. (8) we get

$$0 = \sum_{j=1}^{n}\left\{\left[K_{ij}^e + H_{ij}^e\right] T_j^e - q_i^e - Q_i^e - P_i^e\right\}$$

where,

$$K_{ij}^e = \int_{\Omega^e}\left\{k \frac{\partial \psi_i^e}{\partial x} \frac{\partial \psi_j^e}{\partial x} + k \frac{\partial \psi_i^e}{\partial y} \frac{\partial \psi_j^e}{\partial y} + C \psi_i^e \psi_j^e\right\} dxdy$$

$$H_{ij}^e = \oint_{\Gamma^e} \beta \psi_i^e \psi_j^e ds$$

$$q_j^e = \int_{\Omega^e} f \psi_i^e dxdy$$

$$P_i^e = \oint_\Gamma \psi_i^e q_n \, ds$$

$$Q_i^e = \oint_\Gamma \psi_i^e \beta T_\infty \, ds$$

In matrix notation the finite element model can be expressed as

$$[K][T] = [Q] + [q] + [P] \tag{8}$$

where, $[K]$ is the conductivity matrix and right hand side is a vector.

We solve equation (8) by iterative method.

3. NUMERICAL RESULTS AND DISCUSSION

Our skin model is 5.325 mm along the X-axis and 7 mm along the Y-axis. Our finite element model contains three layers. Each layer has distinctive material properties. Along the X-axis, $\Omega_1 = 0.075$mm is the epidermis portion, $\Omega_2 = 1.5$mm is the dermis, and the remaining Ω_3 is the subcutaneous tissue. The heating disk is placed 5.5 mm along Y-axis and 1.5 mm is considered a natural convection to ambient air and evaporation boundary. Table 1 shows the properties of materials and parameters [12,15,16].

Table 1: The parameters used in this investigation and their values.

Parameter	Symbol	Value
Thermal conductivity: Epidermis Dermis Sub-Cutaneous tissu	k	0.21 W/m^2 0.37 W/m^2 0.16 W/m^2
Blood Perfusion: Epidermis Dermis Sub-Cutaneous tissue	ω_b	0 ml/s/ml 0.00125 ml/s/ml 0.00125 ml/s/ml
Density of Blood	ρ_b	1100 kg/m^3
Specific heat of blood	c_b	3300 Jkg^{-10}C^{-1}
Evaporation Rate	E	10 W/m^2
Temperature of the artery	T_α	34 °C
Heat convection coefficient	h_b	7 W/m^2°C
Environmental temperature	T_0	25 °C

The analytical solution of Pennes bio-heat equation in two dimensions is very difficult to obtain. That is why, to test our two-dimensional computer code, we developed a similar model of the problem in COMSOL-Multiphysics [17], which is a general-purpose software platform based on advanced numerical methods for modelling and simulating physics-based problems. We have compared our result with the result obtained from COMSOL Multiphysics. Fig.3 and Fig.4 show that our result is very close to the COMSOL Multiphysics result. So, the computer code and the solution procedure are reliable for further study. Typical tissue properties used in this section are given in Table 1. We also compare our computed result with the one-dimensional analytical solution found in [18]. In Fig. 5, you can see that our computed result is exactly the same as the analytical result.
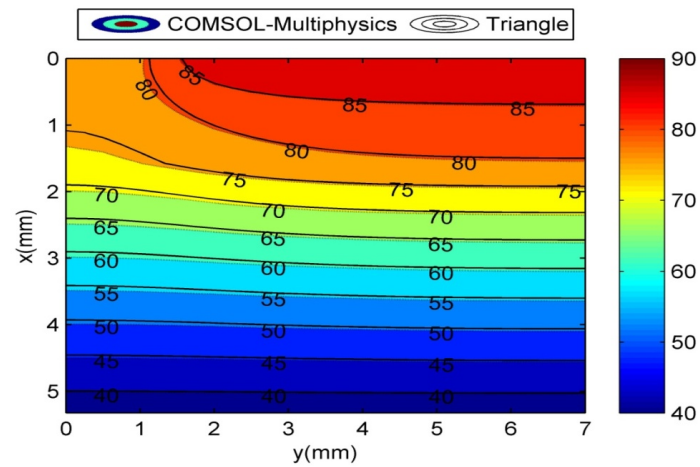
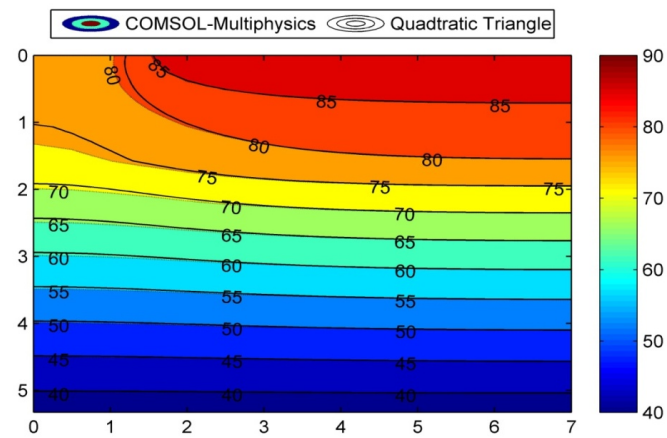**Fig. 3 Comparison results of triangle and COMSOL- Multiphysics.**

Fig. 4 Comparison results of quadratic triangle and COMSOL-Multiphysics.
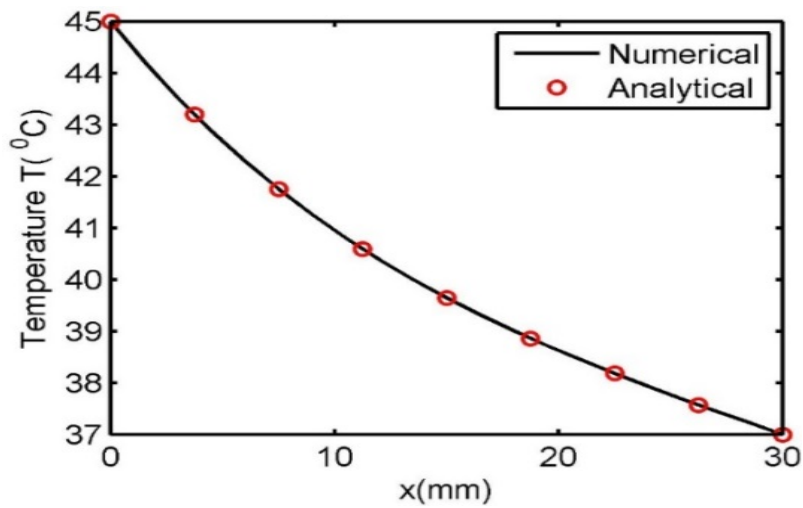

Fig. 5 Comparison with analytical result.

In order to determine the severity of the burn, the temperature distribution within the solution domain was examined using various values of parameters, specifically the thermal conductivity of the skin's outmost layer (epidermis), dermis, and subcutaneous fat, the temperature of the heating disk, the ambient temperature, the convection coefficient of the ambient, the sweat rate of evaporation, and the rate of blood perfusion. Identification of the impacts of a single parameter on the spreading heat inside the skin tissue throughout the burn process is the goal of this investigation, also known as a sensitivity analysis.
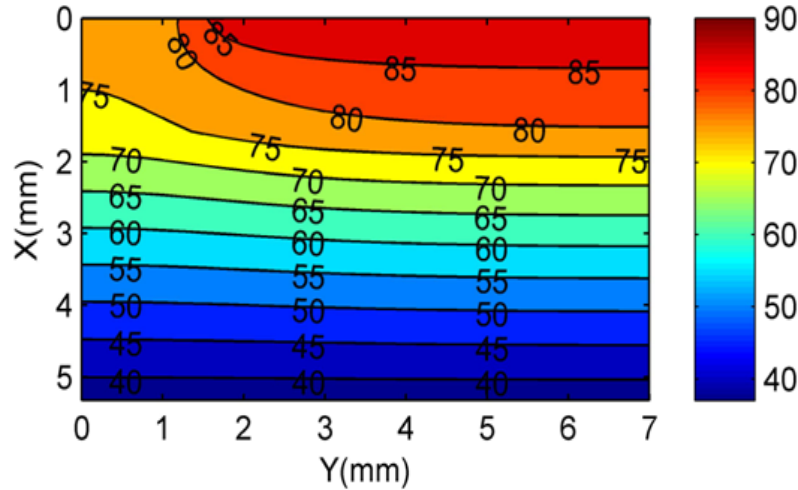

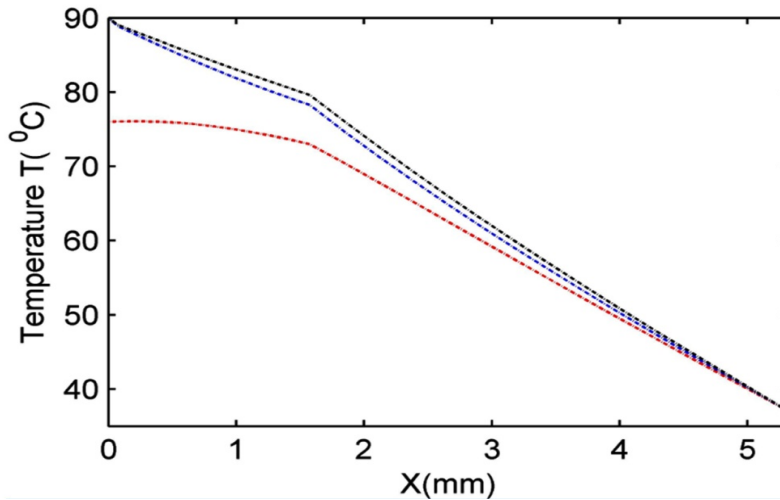**Fig. 6 Steady state temperature distribution in human skin.**

Fig. 7 Temperature distributions along x-axis. Red line, y = 0 mm; Blue line, y = 3 mm; and Black line, y = 7 mm.

Fig. 6 shows how the temperature changes in the human skin model based on the values of the parameters in Table 1. The surface on which the heating disc is placed gets the hottest (shown in red). The skin's base (seen in blue) has the lowest temperature, which is equal to the body's core temperature of 37^0C. In Fig. 6,

the solid lines show where the isotherms are in the human skin. The surface temperature of the epidermis dropped to the environment, which was determined to be around 75^0C. As a result, people's skin may have been exposed to the environment. Heat is transferred from the heating disc into the skin as it comes into contact with the skin. Convection and evaporation from the epidermis's surface transport the extra heat to the surrounding air. Moreover, the dermal blood flow acts as a medium to dissipate the extra heat generated by the skin tissue.

The temperature profile is depicted in Fig. 7 along the x-axis at y = 0 mm, y = 3 mm, and y = 7 mm. These y values were chosen to give a more accurate picture of how the skin temperature is spread out. In the area where the subcutaneous fat is located, the skin's warmth seems to rise uniformly. When y = 3 mm and y = 7 mm, a sharp increase is seen inside the dermis. This could be a result of the area being so close to the heating disk. Due to heat loss from the outer part of the skin to the ambient, the rate of temperature rise decreases at y = 0 mm.

3.1 Sensitivity analysis

Here a sensitivity analysis is performed as a key method for examining how behave in the various skin parameters during burns can impact the distribution of skin temperature. Variables are categorized with the greatest impact on human skin epidermis layer. The severity of thermal injury to the skin is proportional to the temperature rise, so it is important to evaluate the clinical importance of each variable

In this specific analysis, eight parameters are taken into account. Included among these are "the thermal conductivity of the epidermis, dermis, and subcutaneous fat, the temperature of the disc, the rate of blood perfusion, the ambient convection coefficient, the ambient temperature, and the rate of skin surface evaporation" [19]. The values of each of these factors are adjusted slightly from the control level in order to study how changes in each of them might alter the distribution of skin temperature (table 1). Other parameters' values should be held constant while each parameter is investigated. It is expected that there will be two alternative values, one of which is higher and the other lower than the control value. At y = 0, 3, and 7 mm, observations are made along the x-axis.

3.1.1 Epidermis thermal conductivity's impact

0.21Wm^{-1} K^{-1} is chosen as the control value for the epidermal thermal conductivity. In actual life, the heat conductivity of each individual and different body parts varies. Due to this, 0.105 and 0.42 Wm^{-1}K^{-1}, which are lower and higher than the control value, respectively, were deemed two values. All of these values' effects are observed.

The findings of the investigation are displayed in Fig. 8. Variations in the epidermis' heat conductivity appear to have relatively little impact on how hot or cold the human skin is inside. This might be because the epidermis has a relatively thin structure, which makes any changes in heat conductivity have a negligible effect on the system's overall temperature sensitivity. This study's findings show that, when analyzing skin damage, the epidermis will likely incur the most damage. This is because the heat from the heating disk was transferred directly over this layer.
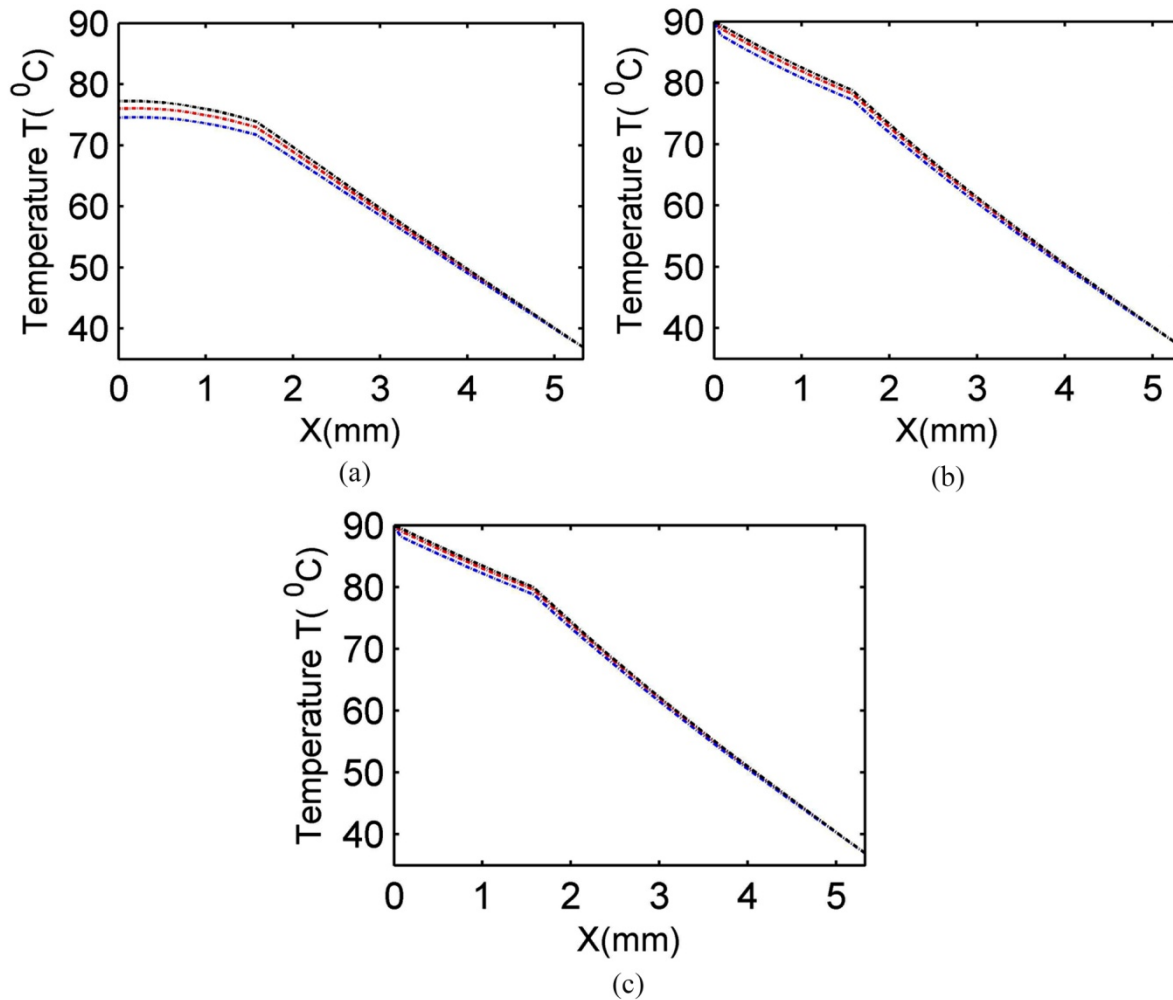
Fig. 8 Effect of Epidermis thermal conductivity. (a) y = 0 mm, (b) y = 3.5 mm and (c) y = 7 mm. Red lines, *k* = 0.21; Black lines, *k* = 0.42; and Blue lines, *k* = 0.105.

3.1.2 Effect of dermis thermal conductivity

The dermis thermal conductivity is investigated using the same justification as the epidermis thermal conductivity. Values of 50 percent and 200 percent of the control are investigated.
Both of these numbers are equivalent to 0.185 and 0.74 Wm1 K1. The outcomes are displayed in Fig. 9. It is apparent that the dermis, whose heat conductivity is higher, has a higher internal temperature. Variations in the dermis' heat conductivity have a less significant impact on how hot or cold the skin is within.

3.1.3 Subcutaneous fat thermal conductivity's impact

The thermal conductivity of subcutaneous fat is given by values of 0.08 and 0.32 W/m2K1, respectively, equivalent to 50 and 200 percent of the control. Fig. 10 shows the numerical results that were achieved. According to Fig. 10, an increase in subcutaneous fat thermal conductivity results in a modest drop in temperature at the point where the dermis layer and subcutaneous fat meet (y = 1.5mm). In other words, a lower tissue temperature is found from a higher fat thermal conductivity. The skin tissue can cool down more quickly with better heat conductivity, causing less tissue injury.
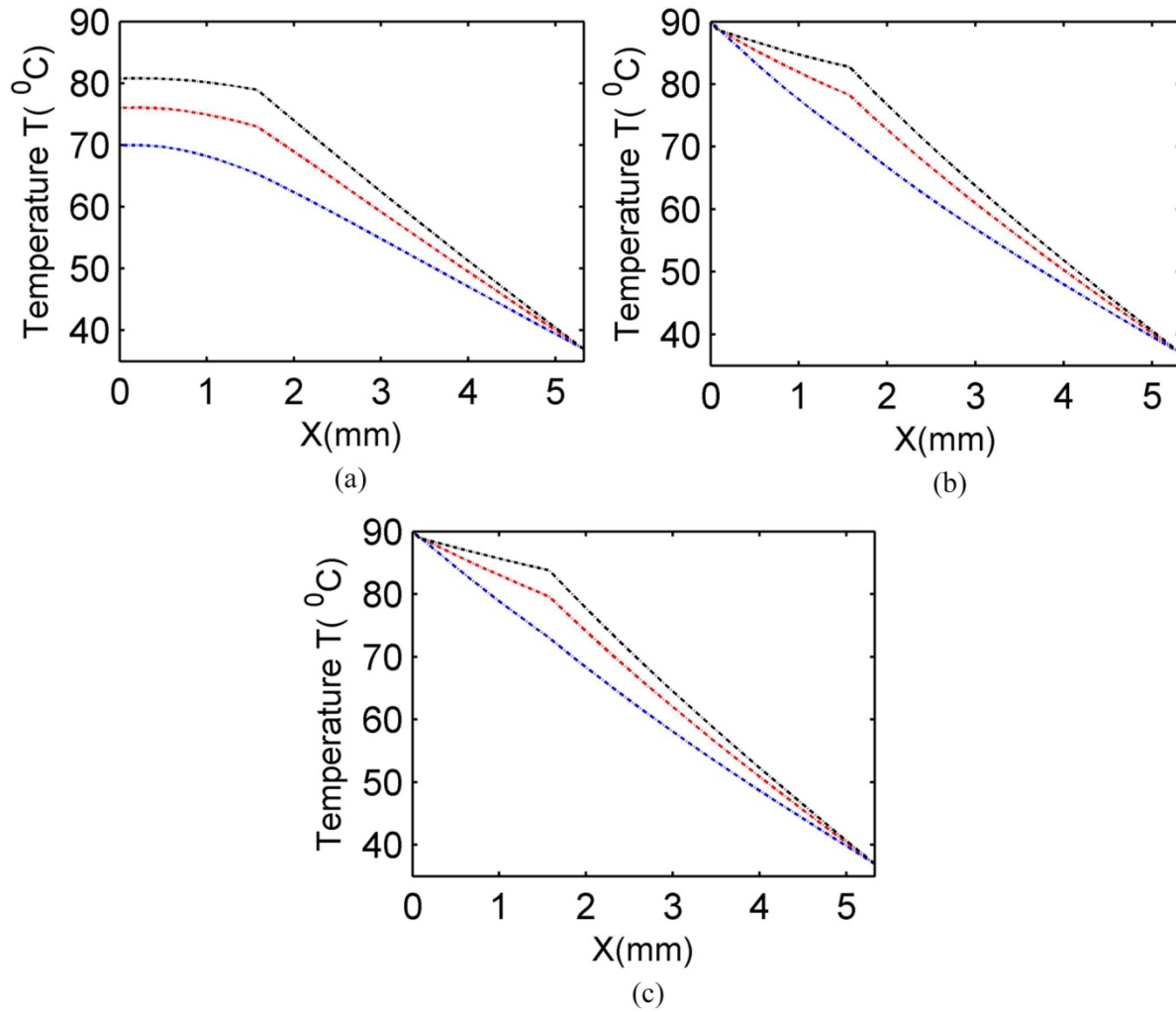
(a)

(b)

(c)

**Fig. 9 Effect of dermis thermal conductivity. (a) y = 0 mm, (b) y =3.5 mm and
(c) y = 7 mm. Red lines, k = 0.37; Black lines, k = 0.74; and Blue lines, k = 0.185.**

3.1.4 Effect of disk temperature

To examine the impact of the temperature distribution inside the human skin during continuous heating burn, two distinct values 60^0C and 120^0C that are fewer and larger than the control value, respectively, are chosen. Fig. 11 presents the findings in graphic form. In contrast to the changes at y = 0 mm, this figure shows that the skin temperature at y = 3 mm and 7 mm exhibits a little thermal variation. This is not surprising because the areas along y = 3 mm and 7 mm are where the heat originates, whereas at y = 0 mm, cooling occurs at the skin's surface, where it is exposed to the environment. We see that the skin tissue closest to the body's core has the lowest temperature, and that the surface to which the heating disk is attached has the highest temperature. The higher temperatures shown by the lines indicate that the disk temperature is higher. Considering that the heat supply from the hot disk is primarily distributed to the surroundings by convection and sweat evaporation, it also appears that the core temperature of 37^0C is smaller than the temperature at the convection surface. Furthermore, because the epidermal layer is so thin, there is no discernible change in temperature (only 0.075 mm).
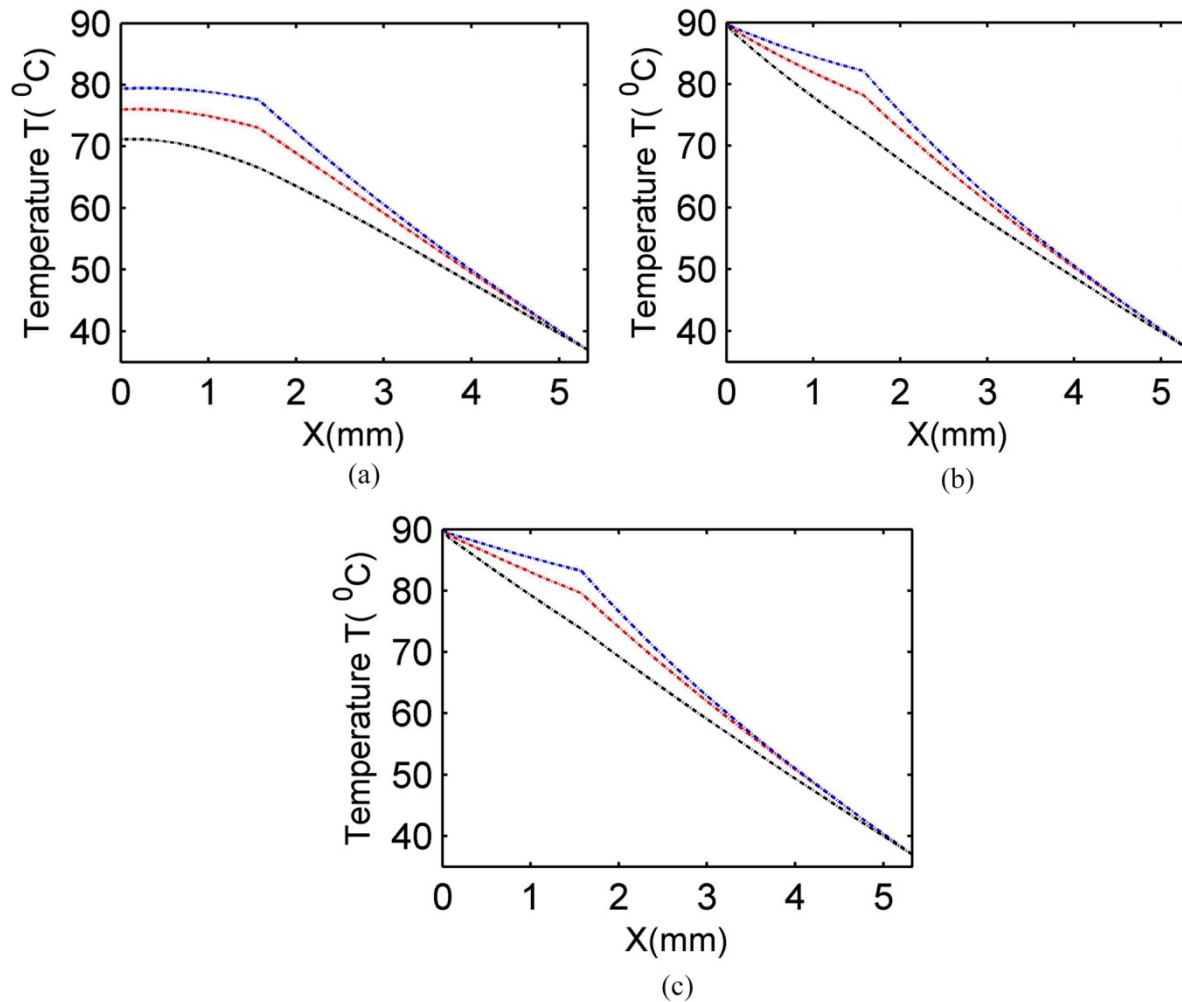
Fig. 10 Effect of subcutaneous fat thermal conductivity. (a) y = 0 mm, (b) y = 3.5 mm and (c) y = 7 mm. Red lines, *k* = 0.16; Black lines, *k* = 0.32; and Blue lines, *k* = 0.08.

3.1.5 Rate of blood perfusion's effect

The values of perfusion rate are 0.0005 ml/s/ml, 0.00125 ml/s/ml, and 0.024 ml/s/ml, where 0.00125 ml/s/ml is assumed to be a control value and the other two are considered lower and higher values of control. This is done to examine the effect of the blood perfusion rate inside the skin during the temperature distribution. Fig. 12 depicts how the rate of blood circulation within the skin affects the distribution of temperature. Higher blood perfusion rates have been observed to reduce skin temperature. When the body's tissue temperature rises, the blood vessels immediately dilate, and the blood flow increases, decreasing the amount of heat that builds up in the body and lessening tissue damage. Hence, when the rate of blood perfusion rises, the average heat of tissue decreases. The findings shown in fig. 3.10 tell us that boosting the flow of blood within the tissue can aid in transporting the extra heat away, thereby reducing burn damage to the skin.
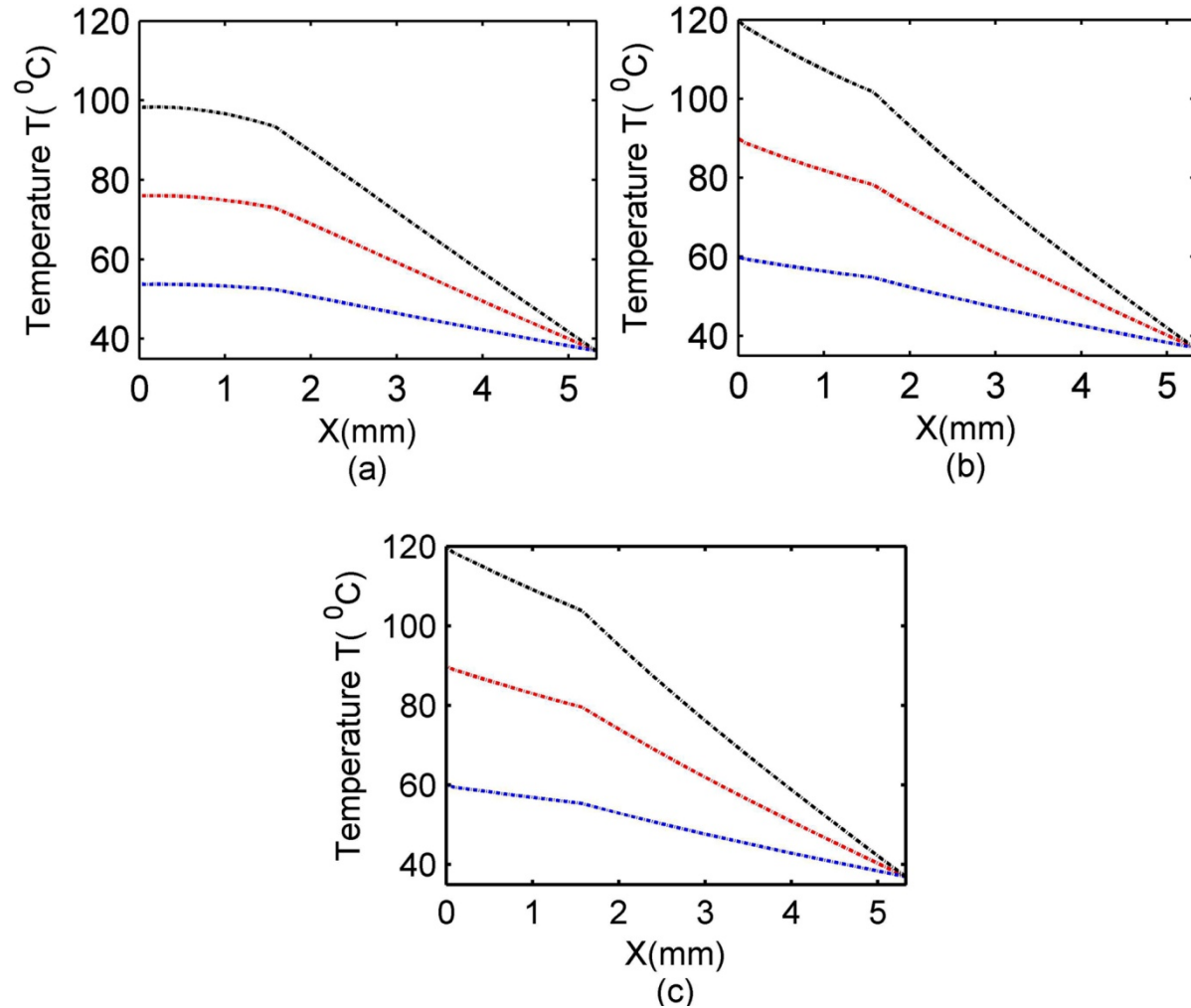
Fig. 11 Effect of disk temperature. (a) y= 0 mm, (b) y = 3 mm and (c) y = 7 mm.
Red lines, T_d= 90ºC; Black lines, T_d = 120ºC; and Blue lines, T_d = 60ºC.

3.1.6 Effect of ambient heat transfer coefficient

Investigations are made into how ambient convection coefficient affects burns within human skin. The ambient convection coefficient's control value is $7Wm^{-2} K^{-1}$. This value suggests that the skin surface is experiencing natural convection. As the transition from natural to forced convection begins, we will take into account values of $25Wm^{-2} K^{-1}$ and $250Wm^{-2} K^{-1}$, respectively.

It is expected that the ambient temperature is 25^0C. Outcome visualization is shown in Fig. 13. This graph shows that the convection coefficient has almost no effect of temperature spread within the skin at y = 7mm. Yet, at the convection surface of the skin at y = 0 mm, we observed a considerable impact on temperature distribution. where the convection coefficient rises and the temperature drops considerably. The results indicated that heat harm could be avoided in clinical situations by promoting convection at the skin's surface
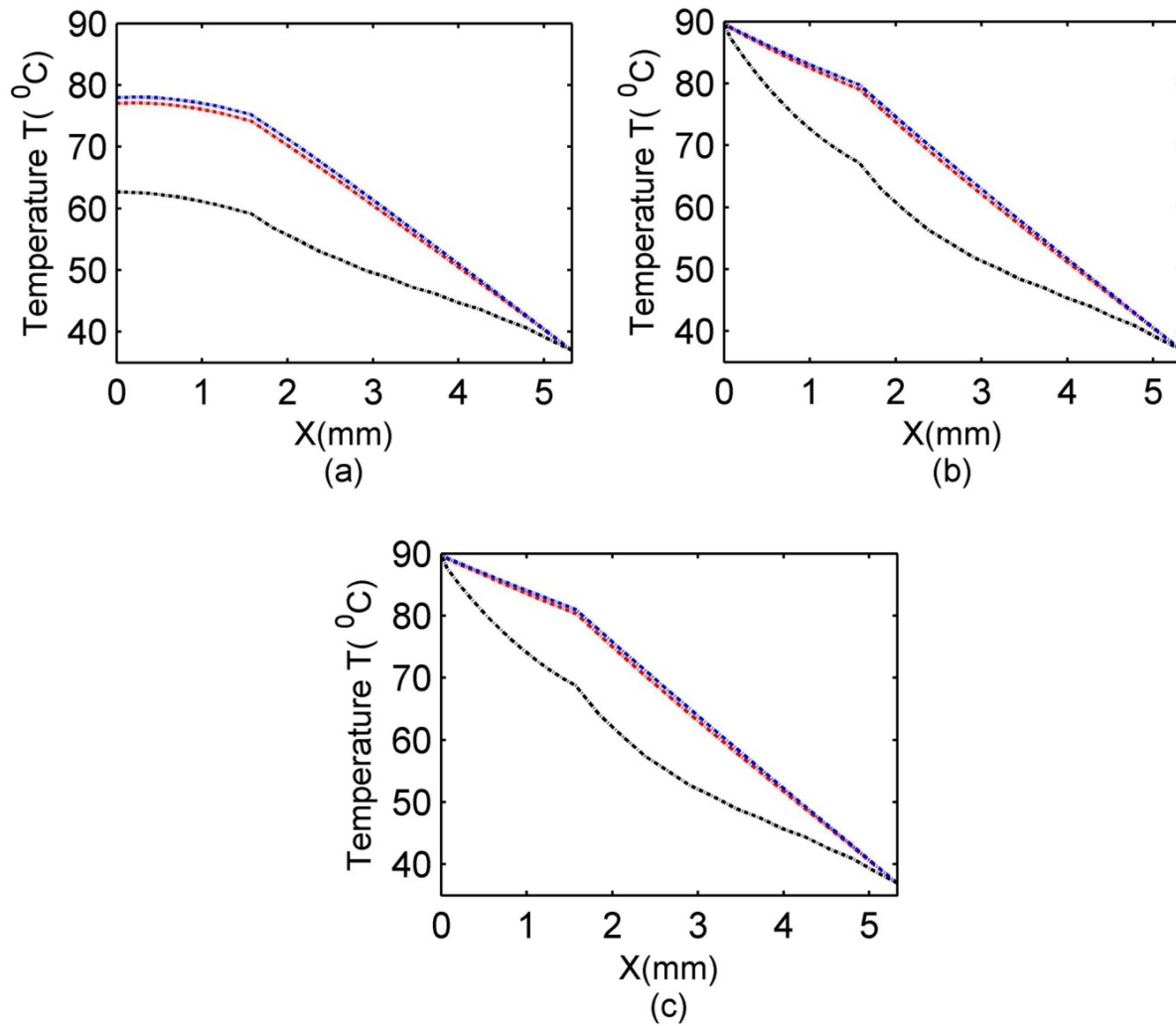
Fig. 12 Effect of blood perfusion rate. (a) y = 0 mm, (b) y = 3 mm and(c) y = 7 mm.
Red lines, w_b= 0.00125 ml/s/ml; Black lines,w_b = 0.024 ml/s/ml; and
Blue lines,w_b = 0.0005 ml/s/ml.

3.1.7 Effect of ambient temperature

As a control value, we used an ambient temperature of 25^0C. To examine the impact of internal skin temperature during a burn. We take into account two temperatures, 16^0C and 40^0C, which are respectively lower and higher than the control value. The findings, which are shown in Fig. 14, demonstrate that there is little difference in the distribution of temperature within the skin between different ambient temperatures. This shows that plummeting the temperature of the ambient would not be a smart strategy to reduce the chance of damage to burn victims' skin.

3.1.8 Effect of skin evaporation rate

10W/m^{-2} is used as the control value for sweat evaporation rate. The evaporation rate values show how much heat is lost as a result of sweat leaving the skin of people. Values of 0 and 15Wm^{-2} are chosen to

examine how small and larger values may alter the distribution of temperature within the skin. The outcomes are shown in Fig. 15. The different evaporation rate values have almost no impact on how hot or cold the skin is. This is expected to account for only about 15% of the total heat loss due to evaporation from the skin's surface. Perhaps there would be some noticeable effects from a higher evaporation rate.
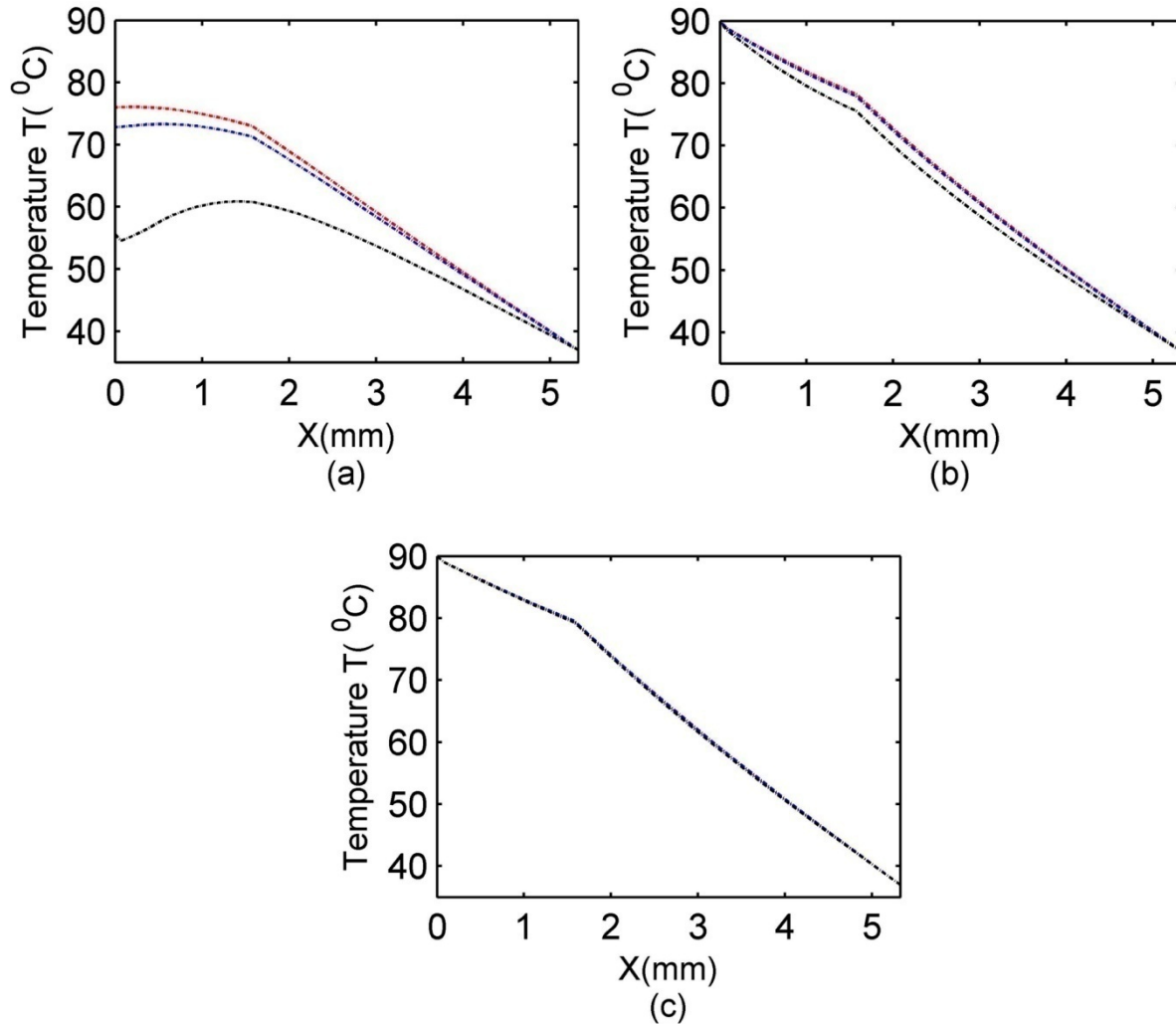

Fig. 13 Effect of ambient convection coefficient. (a) y = 0 mm, (b) y = 3 mm and(c) y = 7 mm. Red lines, h **= 7Wm^{-2} K^{-1}; Black lines,** h **= 250Wm^{-2} K^{-1}; and Blue lines,** h **= 25Wm^{-2} K^{-1}.**

Fig. 14 Effect of ambient temperature. (a) y = 0 mm, (b) y = 3 mm and(c) y = 7mm. Red lines, T_0= 25⁰C; Black lines,T_0 = 40⁰C; and Blue lines T_0 = 16⁰C.

Fig. 15 Effect of evaporation rate. (a) y = 0 mm, (b) y = 3 mm and(c) y = 7 mm.
Red lines, E = 10Wm^{-2}, Black Lines, E = 15Wm^{-2}and Blue lines, E = 0 Wm^{-2}.

CONCLUSION

The steady state temperature profile of human skin is studied using our two-dimensional Finite Element (FE) model of human skin in contact with a heating disk. Since our results and the results from COMSOL-Multiphysics are in good agreement, this model can be used for more research. For the same mesh grid, results are calculated for both linear and quadratic triangular elements. Although there isn't a lot of noticeable variation in the outcome, there is a difference in the computational work. As opposed to 1008 quadratic triangular elements, 4032 linear triangular elements are required for the same mesh grid. Thus, adopting quadratic elements results in less computational work and faster processing. Our findings can be used to create an outline of a burn condition that might actually occur. We demonstrated different properties of human skin have significant effect of temperature distribution inside the different layers of skin. Our findings can be applied to determine the burn intensity in real-world scenarios. This model can be extended in three dimensional for steady and unsteady temperature distribution in human skin model.

REFERRENCES

[1]   WHO Burns fact sheet. [http://www.who.int/mediacentre/factsheets/fs365/en/]

[2]   P. D. Maguire, T. V. Samulski, L. R. Prosnitz, E. L. Jones, G. L. Rosner, B. Powers,
        L.Layfield, D. M. Brizel, S. P. Scully, J. M. Harrelson and M.W. Dewhirst. A phase II trial testing
        the thermal dose parameter CEM43° T 90 as a predictor of response in soft tissue sarcomas treated
        with pre-operative thermos radio therapy, International Journal of Hyperthermia, 2001, 17(4), pp.
        283-290.

[3]   F. C. Henriques and A. R. Moritz. Studies of thermal injury: I. The conduction of heat to nd through
        skin and the temperatures attained therein. A theoretical and an
        experimental investigation, The American journal of pathology, 1947, 23(4), pp. 530-549.

[4]   K. Buettner. Effects of extreme heat and cold on human skin. II. Surface temperature, pain and heat
        conductivity in experiments with radiant heat, Journal of Applied Physiology, 1951, 3(12), pp. 703-
        713.

[5]   H. H. Pennes. Analysis of tissue and arterial blood temperatures in the resting human
        forearm, Journal of Applied Physiology, 1948, 1(2), pp. 93-122.

[6]   E. Y. K. Ng, H. M. Tan and E. H. Ooi. Boundary element method with bioheat equation
        for skin burn injury, Burns, 2009, 35(7), pp. 987-997.

[7]   K. R. Diller. and L. J. Hayes. Analysis of tissue injury by burning: comparison of in situ   and skin
        flap models, International Journal of Heat and Mass transfer, 1991, 34(6), pp.1393-1406.

[8]   H. Wang and Q.-H. Qin. A fundamental solution-based finite element model for analyzing multi-
        layer skin burn injury. Journal of Mechanics in Medicine and Biology, 2012. 12(5),1250027.

[9]   E. Y. K. Ng and L. T. Chua. Prediction of skin burn injury. Part 1: Numerical modelling,
             Proceedings of the Institution of Mechanical Engineers, Part H: Journal of Engineering in
        Medicine, 2002, 216(3), pp. 157-170.

[10]   B. L. Viglianti, M. W. Dewhirst, J. P. Abraham, J. M. Gorman and E. M. Sparrow.
        Rationalization of thermal injury quantification methods: Application to skin burns,
        Burns, 2004, 40(5), pp. 896-902.

[11]   A. M. M. Mukaddes, R. Shioya, M. Ogino, D. Roy, & R. Jaher. Finite element- based analysis of
        bio-heat transfer in human skin burns and afterwards. *International Journal of Computational
        Methods*, 2021, *18*(3), p.2041010.

[12]   S. Mridul, A. M. M. Mukaddes, R. Md Matiar, M.A.H. Mithu. Analysis of the effect of external
        heating in the human tissue: A finite element approach. Polish journal of Medical physics and
        engineering; Warsaw Vol. 26, Iss, 4, (2020), pp. 251-262.

[13]   S. Wahyudi and F. Gapsari. Analysis of Temperature Distribution of Human Skin Tissue in Various Environmental Temperature with the Finite Volume Method. International Journal of Mechanical Engineering and Robotics Research. 2022 Jan 1;11(2), pp.99-105.

[14]   S. Chakraverty, N. Mahato, P. Karunakar, T. Rao. Weighted Residual Methods.1st Ed. Udicha, India: Wiley Telecom, 2019.

[15]   K. R. Diller and L. J. Hayes. A finite element model of burn injury in blood-perfused skin, Journal of Biomechanical Engineering, 1983, 105(3), pp. 300-307.

[16]   D. A. Torvi and J. D. Dale. A finite element model of skin subjected to a flash fire, Journal of biomechanical engineering, 1994, 116(3), pp. 250-255.

[17]   Open source, https://www.comsol.com/product-download/5.6/windows.

[18]   Z. -S. Deng and J. Liu. Analytical study on Bioheat transfer problems with spatial or transient heating on skin surface or inside biological bodies, Journal of Biomechanical Engineering, 2002,124(6):638-649.

[19]   E. Y. K. Ng, H. M. Tan, and E. H. Ooi. Prediction and parametric analysis of thermal profiles within heated human skin using the boundary element method, Philosophical Transactions of the Royal Society A Mathematical, Physical and Engineering Sciences, 2010, 368(1912), pp. 655-678.

Nomenclature

ρ: density of tissue
c: specific heat of tissue
ρ_b: density of blood
c_b: specific heat of blood
k: Thermal Conductivity of tissue.
T_∞: Ambient temperature.
Q_r: External Heating.
Q_m: Internal heat generation (Metabolism.)
T: Unknown Tissue Temperature.
T_a: Arterial temperature (37^0C)
T_c: Body core temperature (37^0C)
T_f: Surrounding Fluid Temperature.
h_b: Convection heat transfer coefficient.
E: Evaporation rate.
σ: Stefan Boltzmann constant
h_b : Convection coefficient.
ω_b : Blood perfusion
δ : Iterative Tolerance